ResearchGate

See discussions, stats, and author profiles for this publication at: https://www.researchgate.net/publication/230712957

Kinetically Blocked Stable Heptazethrene and Octazethrene: Closed-Shell or Open-Shell in the Ground State?

ARTICLE *in* JOURNAL OF THE AMERICAN CHEMICAL SOCIETY · AUGUST 2012

Impact Factor: 12.11 · DOI: 10.1021/ja304618v · Source: PubMed

CITATIONS
62

READS
79

17 AUTHORS, INCLUDING:

Juan Teodomiro López Navarrete
University of Malaga
334 PUBLICATIONS **5,152** CITATIONS
SEE PROFILE

Dongho Kim
Yonsei University
496 PUBLICATIONS **13,380** CITATIONS
SEE PROFILE

Atsuhiro Osuka
Kyoto University
654 PUBLICATIONS **16,435** CITATIONS
SEE PROFILE

Juan Casado
University of Malaga
226 PUBLICATIONS **3,637** CITATIONS
SEE PROFILE

Available from: Yuan Li
Retrieved on: 17 January 2016

JACS
JOURNAL OF THE AMERICAN CHEMICAL SOCIETY
Article
pubs.acs.org/JACS

Kinetically Blocked Stable Heptazethrene and Octazethrene: Closed-Shell or Open-Shell in the Ground State?

Yuan Li,[†] Wee-Kuan Heng,[†] Byung Sun Lee,[‡] Naoki Aratani,[§] José L. Zafra,[∥] Nina Bao,[⊥] Richmond Lee,[#] Young Mo Sung,[‡] Zhe Sun,[†] Kuo-Wei Huang,[#] Richard D. Webster,[¥] Juan T. López Navarrete,[∥] Dongho Kim,*[,‡] Atsuhiro Osuka,*[,§] Juan Casado,*[,∥] Jun Ding,*[,⊥] and Jishan Wu*[,†,▽]

[†]Department of Chemistry, National University of Singapore, 3 Science Drive 3, 117543, Singapore

[‡]Spectroscopy Laboratory for Functional π-Electronic Systems and Department of Chemistry, Yonsei University, Seoul 120-749, Korea

[§]Department of Chemistry, Graduate School of Science, Kyoto University, Sakyo-ku, Kyoto 606-8502, Japan

[∥]Department of Physical Chemistry, University of Malaga, Campus de Teatinos s/n, 229071 Malaga, Spain

[⊥]Department of Materials Science & Engineering, National University of Singapore, 119260, Singapore

[#]Division of Chemical and Life Sciences and Engineering and KAUST Catalysis Center, King Abdullah University of Science and Technology (KAUST), Thuwal 23955-6900, Saudi Arabia

[¥]Division of Chemistry & Biological Chemistry, School of Physical & Mathematical Sciences, Nanyang Technological University, 21 Nanyang Link, 637371, Singapore

[▽]Institute of Materials Research and Engineering, A*Star, 3 Research Link, Singapore, 117602

Supporting Information

ABSTRACT: Polycyclic aromatic hydrocarbons with an open-shell singlet biradical ground state are of fundamental interest and have potential applications in materials science. However, the inherent high reactivity makes their synthesis and characterization very challenging. In this work, a convenient synthetic route was developed to synthesize two kinetically blocked heptazethrene (**HZ-TIPS**) and octazethrene (**OZ-TIPS**) compounds with good stability. Their ground-state electronic structures were systematically investigated by a combination of different experimental methods, including steady-state and transient absorption spectroscopy, variable temperature NMR, electron spin resonance (ESR), superconducting quantum interfering device (SQUID), FT Raman, and X-ray crystallographic analysis, assisted by unrestricted symmetry-broken density functional theory (DFT) calculations. All these demonstrated that the heptazethrene derivative **HZ-TIPS** has a closed-shell ground state while its octazethrene analogue **OZ-TIPS** with a smaller energy gap exists as an open-shell singlet biradical with a large measured biradical character (y = 0.56). Large two-photon absorption (TPA) cross sections ($\sigma^{(2)}$) were determined for **HZ-TIPS** ($\sigma^{(2)}_{max}$ = 920 GM at 1250 nm) and **OZ-TIPS** ($\sigma^{(2)}_{max}$ = 1200 GM at 1250 nm). In addition, **HZ-TIPS** and **OZ-TIPS** show a closely stacked 1D polymer chain in single crystals.

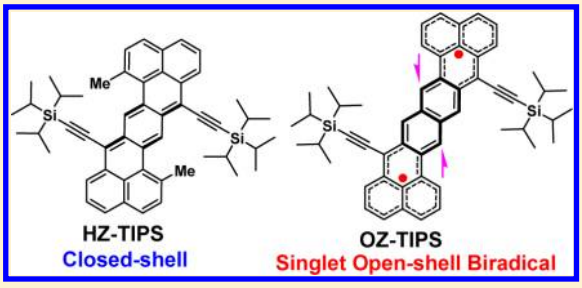

1. INTRODUCTION

Open-shell polycyclic aromatic hydrocarbons (PAHs)[1] are of interest for understanding fundamental chemical and physical phenomenon (e.g., the nature of chemical bonding). In addition, their unique electronic, nonlinear optical (NLO),[2] and magnetic properties make them suitable for functional materials in electronic devices,[3] quantum information processing systems,[4] lithium ion batteries,[5] and organic spintronics.[6] However, the open-shell structure of these molecules renders them vulnerable to degradation reactions; therefore, instability remains a key obstacle for their practical applications. Recent progress in synthetic methods has led to successful synthesis and characterization of several types of stable open-shell PAHs: (1) *p*-quinodimethane[7] and *o*-quinodimethane[8] derivatives, in which the open-shell biradical resonance form contributes largely to the ground-state electronic structure due to the recovery of aromaticity of the quinodimethane unit; (2) phenalenyl[9] and bisphenalenyl[10] derivatives, in which the radicals are thermodynamically stabilized by delocalization throughout the phenalenyl moiety; and (3) low band gap PAHs with Kekulé structure, such as teranthene, in which the breaking of a double bond is compensated by recovery of three Clar's sextet rings.[11] Higher order acenes[12] and periacenes[13] are also predicted to show open-shell character in the ground state, but there is no reported example so far. In most cases, kinetic blocking of the reactive radical sites with bulky groups is necessary to obtain stable materials, even if they are

Received: May 18, 2012
Published: August 21, 2012

 © 2012 American Chemical Society dx.doi.org/10.1021/ja304618v | J. Am. Chem. Soc. 2012, 134, 14913−14922

thermodynamically stabilized by π-electron delocalization or by substitution with electron-withdrawing groups.

Remarkable open-shell biradical character was predicted for the zethrene family, a type of *Z*-shaped PAH which can also be regarded as a dibenzoacene. Theoretical calculations predicted their enhanced static second hyperpolarizability and large two-photon absorption (TPA) cross section.[14] The large biradical character for heptazethrene and octazethrene can be explained by recovery of an aromatic benzene or naphthalene ring in the biradical resonance form, as indicated in Chart 1. Although the

Chart 1. Resonance Structures of Heptazethrene and Octazethrene, and Structures of HZ-TIPS and OZ-TIPS

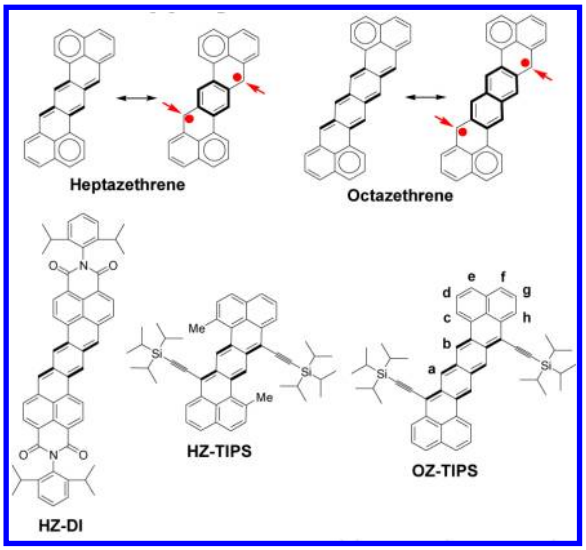

smallest member of the zethrene family, i.e. zethrene, was also predicted to have a significant biradical character, so far all reported zethrene and its derivatives[15] have showed a closed-shell ground state. The synthesis of parent heptazethrene[16] was not successful due to its high reactivity. We recently reported the first synthesis of a heptazethrene derivative, the heptazethrene diimide (**HZ-DI**, Chart 1), and demonstrated that it existed as a singlet open-shell biradical in the ground state.[17] **HZ-DI** showed reasonable photostability in solution; however, the material slowly decomposed during storage either in solution or in solid. The higher order octazethrene[18] and its derivatives have never been reported due to their expected extremely high reactivity. In this paper, we report an efficient synthetic route for a new kinetically blocked heptazethrene derivative (**HZ-TIPS**), in which the most reactive sites (indicated by arrows in Chart 1) are substituted by bulky triisopropylsilylacetylene (TIPS) groups (Chart 1). By using a similar concept, the first stable octazethrene derivative (**OZ-TIPS**, Chart 1), which was found to have a singlet open-shell ground state, was also obtained. The ground-state electronic structures of both compounds were systematically studied by various experiments and density functional theory (DFT) calculations. Their NLO properties and solid-state packing were also investigated in detail.

2. RESULTS AND DISCUSSION

Synthesis and Structural Characterization. Our previous synthetic methods for the zethrene diimide[15f] and heptazethrene diimide[17] using intramolecular transannular cyclization afforded the final products in low yields. Herein, the heptazethrene diketone **4** was chosen as a key intermediate for the high-yield synthesis of **HZ-TIPS** (Scheme 1). Suzuki

Scheme 1[a]

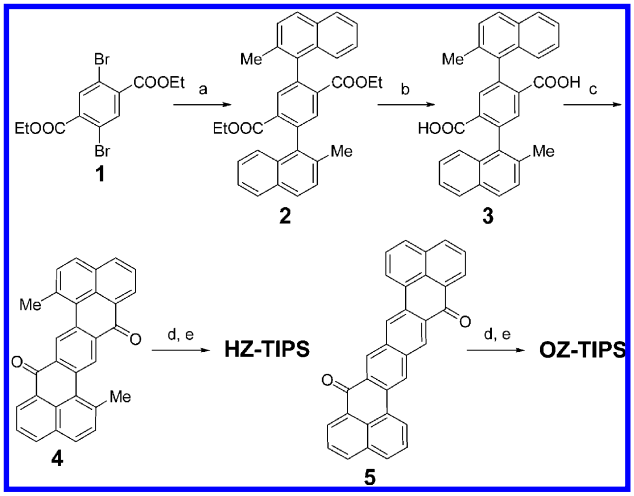

[a]Reagents and conditions: (a) 2-methylnaphthalen-1-yl-1-boronic acid, 3 equiv, $Pd(PPh_3)_4$/ Na_2CO_3, toluene/EtOH, reflux, 82%; (b) NaOH, 8 equiv, THF/MeOH, 70 °C, 95%; (c) PPA, reflux, 93%; (d) *i*-$Pr_3SiC{\equiv}CMgCl$, THF, rt; (e) $SnCl_2$, rt, 2 h; 87% for **HZ-TIPS** and 35% for **OZ-TIPS**, over two steps.

coupling between the diester **1**[19] and 2-methylnaphthalen-1-yl-1-boronic acid[20] followed by acidification of the product **2** gave the diacid **3** in an overall 78% yield. The desired diketone **4** was then obtained from **3** under reflux for 3 h with polyphosphoric acid (PPA). The introduction of a methyl group at the 2-position of the naphthalene moiety prevents the formation of a five-membered ring containing isomers and also improves the solubility of the diketone **4**. Addition of **4** with excessive triisopropylsilylacetylene Grignard reagent followed by reduction with $SnCl_2$ provided **HZ-TIPS** in 87% yield. Using a similar strategy, the octazethrene derivative **OZ-TIPS** was prepared from the corresponding diketone **5**[18] in 35% yield. The structures of **HZ-TIPS** and **OZ-TIPS** were unambiguously identified by 1D ^1H (^{13}C) NMR, 2D NOE/COSY/NOESY NMR spectroscopy, high-resolution mass spectrometry (Figure S1−S10 in the Supporting Information (SI)), and single-crystal analysis (vide infra).

Steady-State and Transient Absorption Spectroscopic Measurements of HZ-TIPS and OZ-TIPS. The solution of **HZ-TIPS** has a blue color and shows a well-resolved one-photon absorption (OPA) spectrum with a *p*-band at 634 nm (Figure 1 and Table 1), which is typical for many closed-shell PAHs, such as rylenes and acenes.[21] **HZ-TIPS** also exhibits a moderate fluorescence quantum yield (16%) with emission maximum at 704 nm (Figure S11 in SI). In addition, **HZ-TIPS** displays a well-resolved ^1H NMR spectrum even under elevated temperatures (e.g., 100 °C in $CDCl_2CDCl_2$, Figure S1 in SI). All these indicate that **HZ-TIPS** likely has a closed-shell structure in the ground state, which is in contrast to its analogue **HZ-DI**, which possesses the same heptazethrene chromophore but with a different substituent.[17] For comparison, **HZ-DI** shows a different absorption band characteristic of a biradicaloid species and there is almost no fluorescence.[17] **OZ-TIPS** has a blue-to-green color and the absorption spectrum displays a well-resolved band in the far-red and near-infrared region, with maxima at 795, 719, 668, and 613

dx.doi.org/10.1021/ja304618v | J. Am. Chem. Soc. 2012, 134, 14913−14922

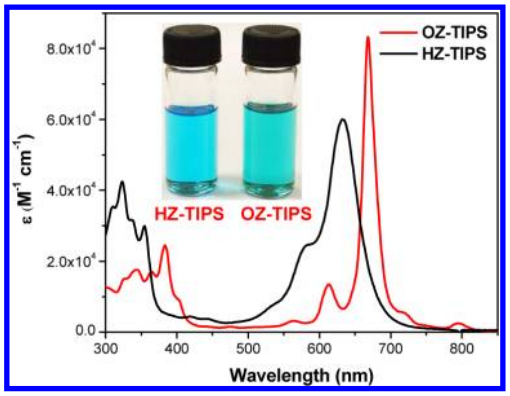

Figure 1. UV−vis−NIR absorption spectra of **HZ-TIPS** and **OZ-TIPS** in chloroform.

nm. The band shape is different from **HZ-TIPS** but is similar to other open-shell PAHs such as teranthene[11] and **HZ-DI**.[17] Moreover, **OZ-TIPS** exhibits a low fluorescence quantum yield of 1.5% with emission maximum at 807 nm (Figure S11 in SI). All these data indicate that **OZ-TIPS** may exist as an open-shell biradical in the ground state, and the lowest energy absorption band likely originates from the presence of a low-lying excited singlet state dominated by a doubly excited electronic configuration (H, H→L, L), as theoretically and experimentally demonstrated by the quinoidal oligothiophene oligomers.[22]

Femtosecond transient absorption (TA) measurements were then carried out to explore the excited-state photophysical properties of **HZ-TIPS** and **OZ-TIPS**. The TA spectra of **HZ-TIPS** and **OZ-TIPS** exhibit ground-state bleach signals around 630 and 670 nm as well as weak excited-state absorption bands in 450−550 and 700−750 nm spectral regions, respectively (Figure 2). The singlet excited-state lifetimes of **HZ-TIPS** and **OZ-TIPS** were estimated to be 3.4 and 1.6 ns, respectively, which are consistent with the fluorescence lifetimes measured by the time-correlated single-photon-counting (TCSPC) technique (Figure S12 in SI). The radiative decay rate constants can be calculated by $k_r = \Phi_f / \tau_f$. Also, because we already know τ_f and k_r, the nonradiative deactivation rate constants can be estimated through $\tau_f = 1/(k_r + k_{nr})$ (Table 1). While the nonradiative decay rate of **OZ-TIPS** was faster than that of **HZ-TIPS**, the radiative decay rate of **OZ-TIPS** was observed much slower than that of **HZ-TIPS**. The difference in the radiative decay rates as well as the nonradiative decay rates between **OZ-TIPS** and **HZ-TIPS** is thought to reflect their respective electronic character.

VT NMR, ESR, and SQUID Measurements. Variable temperature (VT) ^{1}H NMR spectra of **OZ-TIPS** were recorded

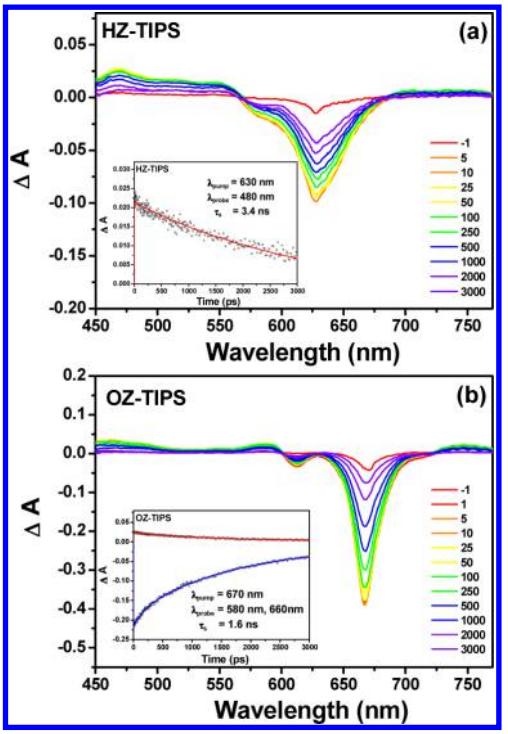

Figure 2. Transient absorption spectra of **HZ-TIPS** (a) and **OZ-TIPS** (b) in chloroform. Insert are the decay curves.

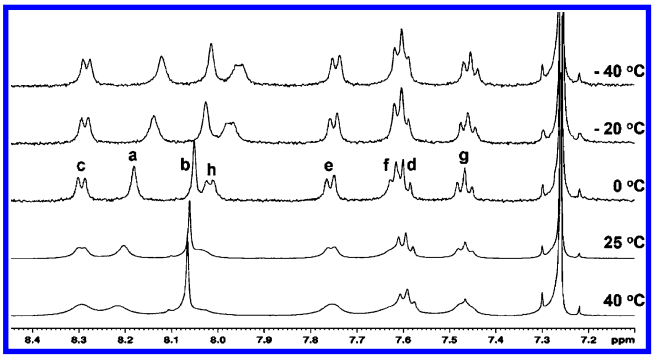

Figure 3. Variable-temperature ^{1}H NMR spectra (aromatic region) of **OZ-TIPS** in $CDCl_3$ and assignment of all aromatic protons. The resonance assignment referred to the structure shown in Chart 1.

in $CDCl_3$ (Figure 3). In contrast to **HZ-TIPS**, the resonances from the octazethrene core in **OZ-TIPS** are significantly broadened at room temperature and further broadened at elevated temperatures. However, these peaks become obviously

Table 1. Photophysical and Electrochemical Data of HZ-DI, HZ-TIPS, and OZ-TIPS[a]

compd	λ_{abs} (nm)	ε_{max} (M^{-1} cm^{-1})	PL (nm)	QY (%)	τ_f (ns)	k_r (s^{-1})	k_{nr} (s^{-1})	$E_{ox}^{1/2}$ (V)	$E_{red}^{1/2}$ (V)	HOMO (eV)	LUMO (eV)	E_g^{EC} (eV)	E_g^{Opt} (eV)
HZ-DI	641, 701, 747, 827	24382	–	–	–	–	–	0.62, 0.93	−0.65, −0.69	−5.22	−4.23	0.99	1.16
HZ-TIPS	584, 634	60000	704	16	3.4	4.7×10^7	2.5×10^8	0.17, 0.69	−1.48, −1.86	−4.87	−3.41	1.46	1.82
OZ-TIPS	613, 668, 719, 795	83300	807	1.5	1.6	9.4×10^6	6.2×10^8	0.02, 0.22, 0.61	−1.30, −1.56, −1.82	−4.73	−3.60	1.13	1.50

[a] λ_{abs}: absorption peak wavelength. ε_{max}: molar extinction coefficient at the absorption maximum. PL: photoluminescence wavelength. QY: fluorescence quantum yield. τ_f: fluorescence lifetime. k_r: radiative decay rate constant. k_{nr}: nonradiative deactivation rate constant. $E_{ox}^{1/2}$ and $E_{red}^{1/2}$ are half-wave potentials of the oxidative and reductive waves, respectively. HOMO and LUMO are determined from the oxidation and reduction onset, respectively. E_g^{EC}: electrochemical energy gap. E_g^{Opt}: optical energy gap.

dx.doi.org/10.1021/ja304618v | J. Am. Chem. Soc. 2012, 134, 14913−14922

sharper as the temperature decreases to 0 °C. This is a typical phenomenon for other PAHs with a singlet open-shell ground state. The NMR signal broadening results from a thermally excited triplet species, which is slightly higher in energy than the singlet biradical state.[10,11,17] Further decrease of temperature led to signal broadening and upfield shift of the resonances of the octazethrene core, particularly for the protons a, b, and h, which can be explained by enhanced aggregation at lower temperature. The existence of strong intermolecular association in solution is supported by the crystallographic analysis to be discussed later on.

Solution and solid powder of **HZ-TIPS** did not show any electron spin resonance (ESR) signal, even at elevated temperatures (up to 400 K), further supporting its closed-shell structure. The solution of **OZ-TIPS** did not show any ESR signal, too; however, its powder exhibited a ESR signal at g = 2.0026 (Figure 4a), and the intensity decreases with a

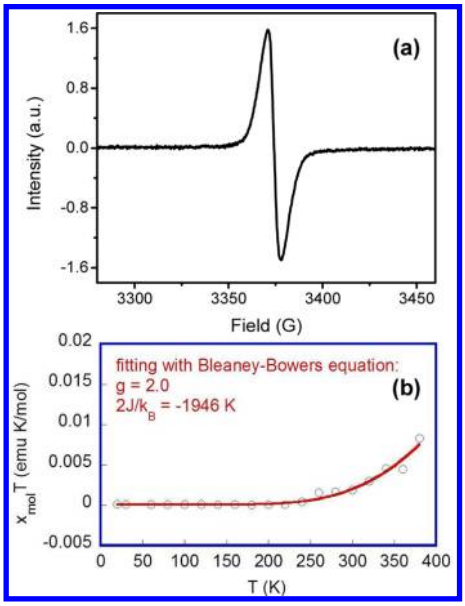

Figure 4. (a) ESR spectrum of **OZ-TIPS** in powder measured at room temperature. (b) $\chi T-T$ plot for the solid **OZ-TIPS**. The measured data was plotted as open circles, and the fitting curve was drawn using the Bleaney–Bowers equation with g = 2.00.

decrease of temperature, presumably due to the lower population of triplet species at lower temperature. However, zero-field splitting and $\Delta m_s = \pm 2$ transition were not observed, probably due to long mean spin–spin separation, and a similar phenomenon was also observed in a *meso*-diketo hexaphyrin biradical.[23] The singlet–triplet energy gap ($\Delta E_{S\text{-}T}$) of **OZ-TIPS** was estimated by superconducting quantum interfering device (SQUID) measurements for a powder sample at 5–380 K. The measurements showed an increasing susceptibility above 220 K (Figure 4b), and careful fitting of the data by using Bleaney–Bowers equation[24] gave a $2J/k_B = -1946$ K (0.168 eV or 3.87 kcal/mol). These measurements prove that **OZ-TIPS** has a singlet open-shell ground state, which can be thermally excited to its triplet excited state at room temperature due to a small singlet–triplet energy gap ($\Delta E_{S\text{-}T} \approx 3.87$ kcal/mol). The percentage of the triplet species at room temperature was thus estimated to be about 0.14%. This also means that there is very low spin concentration in the dilute solution of **OZ-TIPS**, which can explain the ESR silence in solution. However, in the powder form, the increased spin concentration allowed detection of the paramagnetic signal by ESR. SQUID measurement on **HZ-TIPS** only revealed diamagnetism.

FT Raman Spectroscopic Measurements. Raman spectroscopy has proven to be very useful for the characterization of benzene-type aromatic biradicals, either singlets or triplets.[25] This is based on the fact that there exist characteristic benzene vibrational Raman bands around 1600 cm^{-1} that are very sensitive to the electronic configuration within the six-membered benzene ring, either "benzoquinoidal" or "benzoaromatic". Benzoaromatic Raman modes are associated with frequency bands higher than 1600 cm^{-1}, while benzoquinoidal modes always appear at lower frequencies due to the overall CC bond weakening of the benzenoid ring by the loss of aromaticity. Therefore, FT 1064 nm Raman spectroscopy was used to further probe the electronic configuration of the *p*-xylylene and 2,6-naphthodimethane units in **HZ-TIPS** and **OZ-TIPS**.

At room temperature, a diagnostic ν(C=C) band at 1590 cm^{-1} was observed for **HZ-TIPS**, while this band was shifted to 1602 cm^{-1} in **OZ-TIPS** (Figure 5). Such a change could be

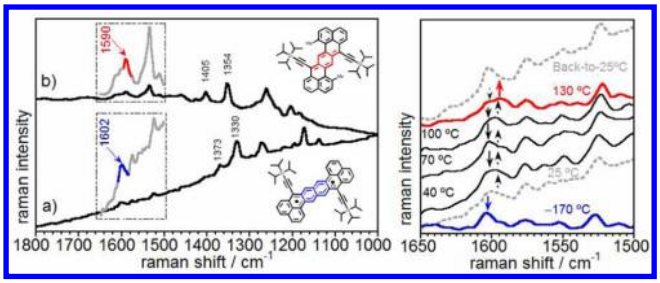

Figure 5. Solid-state 1064 nm FT-Raman spectra of **OZ-TIPS** (a) and **HZ-TIPS** (b) with the regions of interest expanded (left) and variable-temperature Raman spectra of **OZ-TIPS** (right). Arrows highlight the intensity inversion.

explained by the evolution of a *p*-quinodimethane-like structure in the closed-shell **HZ-TIPS** to a pseudoaromatic naphthalene structure in the open-shell **OZ-TIPS** (highlighted in Figure 5).

Variation of temperature did not result in significant change for the Raman spectrum of **HZ-TIPS**. However, for **OZ-TIPS**, thermal heating delineates a progressive 1602/1595 cm^{-1} intensity inversion (Figure 5, indicated by arrow). In the diagnostic 1600 cm^{-1} region, the spectrum displays a single band at 1602 cm^{-1} at −170 °C accompanied by a very weak signal at 1591 cm^{-1}. With the heating of the sample from room temperature up to 130 °C, a band at 1595 cm^{-1} appears and becomes the strongest. Overall the thermal heating leads to a progressive 1602/1595 cm^{-1} intensity inversion, and importantly, the cycle is reversible (i.e., the spectrum is completely recovered by cooling the sample from 130 °C to room temperature). Our recent studies on a viologen sample with similar singlet and triplet biradical forms showed that its triplet form displaced at lower frequency compared with its singlet biradical.[25b] Thus, for **OZ-TIPS**, we can assign the 1602 cm^{-1} band at low temperatures to its singlet biradical species and the downshifted band at 1595 cm^{-1} at 130 °C to its triplet species. By heating, therefore, we promote a singlet-to-triplet intersystem crossing, which is in consistent with the VT NMR, ESR, and SQUID measurements, as discussed above.

To further confirm the assignment, UCAM-B3LYP/6-31G* theoretical calculations of the Raman spectra were conducted

dx.doi.org/10.1021/ja304618v | J. Am. Chem. Soc. 2012, 134, 14913–14922

for the relevant singlet and triplet species of **HZ-TIPS** and **OZ-TIPS** (Figure 6). The main two bands of the theoretical

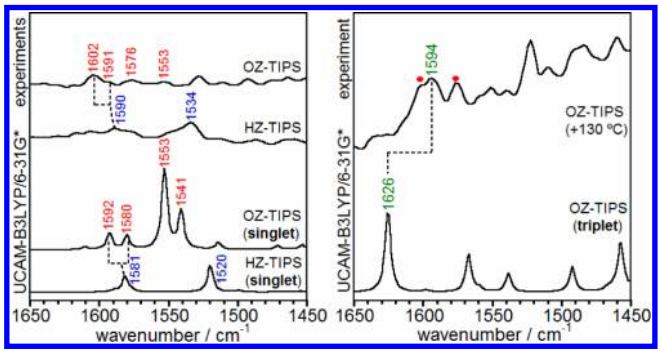

Figure 6. Left: Theoretical UCAM-B3LYP/6-31G* and experimental Raman spectra (in **OZ-TIPS**, the experimental spectrum corresponds to that at −170 °C). Right: UCAM-B3LYP/6-31G* theoretical Raman spectrum of **OZ-TIPS** in its first triplet excited state together with the experimental spectrum at +130 °C. The rest of the bands of the singlet species are denoted as red circles.

spectrum of **HZ-TIPS** at 1581 and 1520 cm^{-1} (difference of 61 cm^{-1}) correlate with the experimental ones at 1590 and 1534 cm^{-1} (difference of 56 cm^{-1}). The band at 1581 cm^{-1} can be described as a CC stretching mode located in the central benzene ring, which represents a motion of the parallel CC bonds of this ring bearing a quinoidal pattern (seen in Figure 7

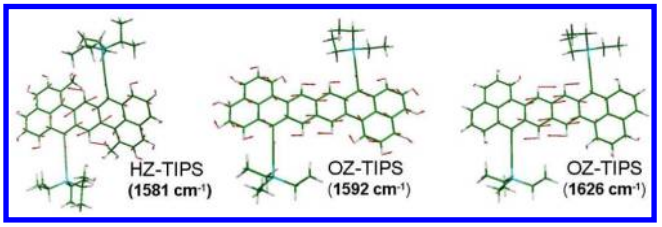

Figure 7. Theoretical vibrational eigenvectors associated with the most relevant bands of the theoretical spectra.

is its theoretical vibrational eigenvector). This 1581 cm^{-1} band splits into two components in **OZ-TIPS** at 1592 and 1580 cm^{-1} (difference of 12 cm^{-1}), which might be related with the experimental bands at 1602 and 1591 cm^{-1} (difference of 11 cm^{-1}). The vibrational eigenvector of the 1592 cm^{-1} theoretical band can be described as a CC stretching placed at the two innermost fused benzene rings in Figure 7. In contrast to that at 1581 cm^{-1} in **HZ-TIPS**, the **OZ-TIPS** mode describes an aromatic-like motion in which the six CC bonds of each benzene vibrate with significant amplitude (in the quinoidal mode this motion is restricted to the parallel quinoidal CC bonds).

Figure 6 also compares the Raman spectrum of **OZ-TIPS** at +130 °C with the UCAM-B3LYP/6-31G* theoretical one of its triplet species. In the 1600 cm^{-1} region, the theoretical spectrum only predicts one intense band at 1626 cm^{-1}. As a result, this theoretical band must be assigned to the sole band that increases its intensity with the heating, that is, the band at 1595 cm^{-1}. The normal mode associated with this band in Figure 7 resembles that associated with the 1592 cm^{-1} band of the open-shell singlet species of **OZ-TIPS**. Therefore, the bands at 1602 and 1591 cm^{-1} measured at −170 °C in **OZ-TIPS** are due to the singlet open shell species. The Raman band of the triplet appears nearby, at 1595 cm^{-1}, but it selectively shows enhancement with the increase of the temperature due to the singlet−triplet equilibrium.

DFT Calculations on the Ground-State Electronic Structures. Unrestricted symmetry-broken DFT calculations using the UCAM-B3LYP method[26] were conducted to further understand the ground-state electronic structures. The $\Delta E_{S\text{-}T}$ values were calculated to be 8.1 and 4.4 kcal/mol for **HZ-TIPS** and **OZ-TIPS**, respectively (triplet above singlet), and the computed energy differences between the closed-shell singlet and the open-shell singlet biradical states were −3.7 and −11.3 kcal/mol for **HZ-TIPS** and **OZ-TIPS**, respectively, suggesting that both molecules may contain a certain degree of the singlet biradical property in the ground state. More informative singlet biradical characters y_0 of 0.159 and 0.434 were obtained for **HZ-TIPS** and **OZ-TIPS**, respectively, to represent their biradical natures between the closed-shell and pure diradical states (0 to 1). While **HZ-TIPS** was predicted to have some lower degree of singlet biradical character in the ground state, our experimental data suggested its closed-shell electronic structure. Such difference between theory and experiment has been observed for other PAHs, especially for those having borderline biradical characters.[27] However, the trends that increasing the conjugated units leads to a decrease of $\Delta E_{S\text{-}T}$ and an increase in the y_0 values are in good agreement with observations in the related systems.[10,11,25b] The calculated singly occupied molecular orbital (SOMO) profiles of the α and β spin of **OZ-TIPS** shown in Figure 8 revealed a typical

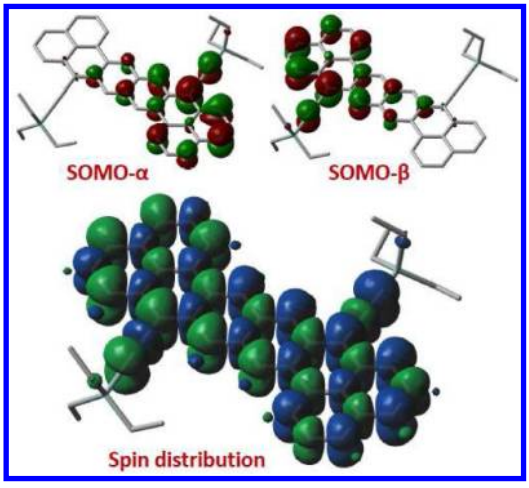

Figure 8. Calculated (UCAM-B3LYP) SOMOs for the α and β electrons and spin density distribution of the singlet biradical of **OZ-TIPS**. Blue and green surfaces represent α and β spin density, respectively. To simplify calculation, the triisopropylsilyl groups are replaced by triethylsilyl units.

disjoint feature, indicating a large singlet biradical character for this molecule. The spin densities in **OZ-TIPS** are evenly distributed throughout the whole octazethrene and ethynylene moieties (Figure 8), which is different from that of the bisphenalenyls, in which the spin density is mainly delocalized at the two terminal phenalenyl units.[10]

TPA Spectroscopic Measurements and Evaluation of the Singlet Biradical Character *y*. As a general rule, we have found that the third-order NLO response reflects variations in the electronic structure as well as the conformational geometry of the molecules, giving rise to the underlying static and dynamic polarizability.[28] In contrast with **HZ-TIPS**, **OZ-TIPS**

dx.doi.org/10.1021/ja304618v | J. Am. Chem. Soc. 2012, 134, 14913−14922

has an unusual ground-state structure with an open-shell configuration, which should be one of the most attractive issues in understanding the TPA−structure correlation between these derivatives. The large TPA activities of bis(phenalenyl) hydrocarbons with benzene and naphthalene spacers possessing an intermediate singlet biradical character have been reported.[2] To characterize NLO properties, the TPA values of **HZ-TIPS** and **OZ-TIPS** were measured by using a wavelength-scanning open aperture *Z*-scan method in the wavelength range from 1200 to 1650 nm, where one-photon absorption contribution is negligible. In relevance to the structure-correlation of radical character, while the TPA cross-section of the closed-shell system **HZ-TIPS** was determined to be 920 GM at 1250 nm, **OZ-TIPS** possessing a singlet biradical character exhibited an enhancement of TPA cross section value of 1200 GM at 1250 nm (Figure 9 and Figure S13 in SI). Such an enhancement on the third-order NLO property can be explained by the larger singlet biradical character of **OZ-TIPS**.

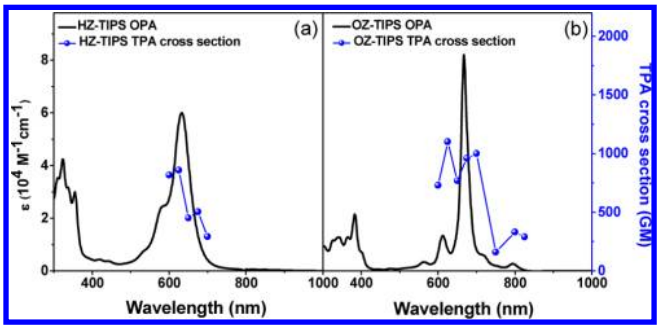

Figure 9. OPA (black solid line and left vertical axis) and TPA spectra (blue symbols and right vertical axis) of (a) **HZ-TIPS** and (b) **OZ-TIPS** in chloroform. TPA spectra are plotted at $\lambda_{ex}/2$.

On the basis of the OPA and TPA data and the $\Delta E_{S\text{-}T}$ value obtained from the SQUID measurement, the singlet biradical character *y* value of **OZ-TIPS** was evaluated to be 0.56 by using the following equation

$$y = 1 - \sqrt{1 - \left(\frac{E_{S_{1u},S_{1g}} - E_{T_{1u},S_{1g}}}{E_{S_{2g},S_{1g}}}\right)^2}$$

where $E_{S_{1u},S_{1g}}$ and $E_{S_{2g},S_{1g}}$ correspond to the energy of the lowest-energy peaks in the one- and two-photon absorption spectra (795 nm = 1.60 eV and 800 nm = 1.55 eV, respectively, in the case of **OZ-TIPS**), and $E_{T_{1u},S_{1g}}$ corresponds to the energy gap between triplet and singlet ground states (3.87 kcal/mol = 0.168 eV for **OZ-TIPS**).[27]

Electrochemical Properties. Cyclic voltammetry was performed to investigate the redox behaviors of **HZ-TIPS** and **OZ-TIPS** (Figure 10, and the data are collected in Table 1). Excellent electrochemical amphotericity was observed for both **HZ-TIPS** and **OZ-TIPS**. **HZ-TIPS** undergoes two reversible oxidations with half-wave potential ($E_{ox}^{1/2}$) at 0.17 and 0.69 V and two reversible reductive waves with half-wave potential ($E_{red}^{1/2}$) at −1.48 and −1.86 V (vs Fc^+/Fc). **OZ-TIPS** shows three reversible oxidation waves with ($E_{ox}^{1/2}$) at 0.02, 0.22, and 0.61 V and three reversible reductive waves with $E_{red}^{1/2}$ at −1.30, −1.56, and −1.82 V (vs Fc^+/Fc). A low electrochemical energy band gap (E_g^{EC}) was determined as 1.13 eV for **OZ-TIPS**, 0.33 eV lower than that of **HZ-TIPS**. For

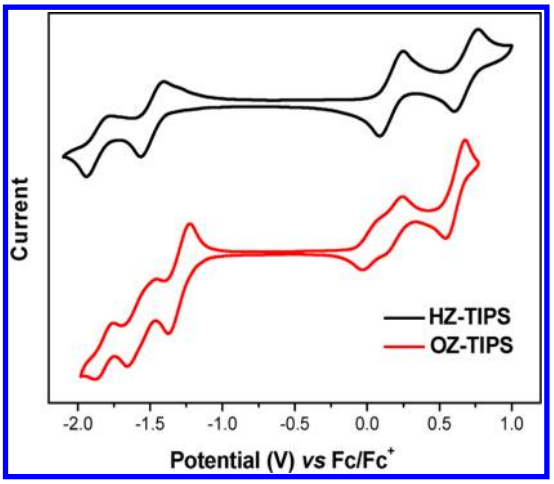

Figure 10. Cyclic voltammograms of **HZ-TIPS** and **OZ-TIPS** in DCM with 0.1 M Bu_4NPF_6 as supporting electrolyte, Ag/AgCl as reference electrode, Au disk as working electrode, Pt wire as counter electrode, and scan rate at 50 mV/s.

comparison, **HZ-DI** has a much smaller E_g^{EC} (0.99 eV) than **HZ-TIPS** (1.46 eV), and the same trend was observed for their optical energy gaps (E_g^{Opt}), i.e, E_g^{Opt} = 1.16 eV for **HZ-DI** and 1.82 eV for **HZ-TIPS** (Table 1). Considering that both **HZ-DI** and **HZ-TIPS** have the same heptazethrene core, such a difference in the energy gap should account for their different ground states. This observation provided further evidence that a small energy gap is a crucial precondition for the formation of a singlet open-shell ground state.[10,11]

X-ray Crystallographic Analysis. Single crystals of **HZ-TIPS** and **OZ-TIPS** suitable for crystallographic analysis were successfully grown from solution and their structure and 3D packing structure determined at 90 K are shown in Figure 11.[29,30] Both molecules are completely flat with point symmetry and exhibit large bond length alternation for the *p*-xylene framework in **HZ-TIPS** and the 2,6-naphthodimethene framework in **OZ-TIPS**. Importantly, the *exo*-methylene double bonds, C2C15 [1.398(2) Å] in **HZ-TIPS** and C3C6 [1.4088(19) Å] in **OZ-TIPS**, are both significantly longer than those in typical olefins (1.33−1.34 A), suggesting the contribution of biradical character. The slightly but distinctly longer *exo*-methylene bond in **OZ-TIPS** is in accordance with their different singlet biradical character.

Interestingly, both **HZ-TIPS** and **OZ-TIPS** are packed into a 1D infinite chain via intermolecular $\pi-\pi$ interactions, with an average π-stacking distance of 3.38 and 3.35 Å, respectively. Such distance is larger than those in the phenalenyl dimer[9] and in the 1D polymer chain of Kubo's bisphenalenyls,[10] in which intermolecular covalent π-bonding is believed to form between the phenalenyl radicals. Thus, the intermolecular interactions in our systems are dominated by $\pi-\pi$ interactions with very less covalent character. Such difference may originate from the closed-shell structure of **HZ-TIPS** and the homogeneous spin distribution in **OZ-TIPS**.

Photostability Test. Compounds **HZ-TIPS** and **OZ-TIPS** remained unchanged in the solid state and in chloroform solution for at least 3 months when stored at 4 °C under nitrogen protection and in the absence of light. In contrast, solid **HZ-DI** decomposed in 1 week under the same conditions. The half-lives of **HZ-TIPS** and **OZ-TIPS** in chloroform upon ambient light irradiation in air at room temperature were found to be as long as 4 days and 34 h, respectively (Figure S14−18 in

dx.doi.org/10.1021/ja304618v | J. Am. Chem. Soc. 2012, 134, 14913−14922

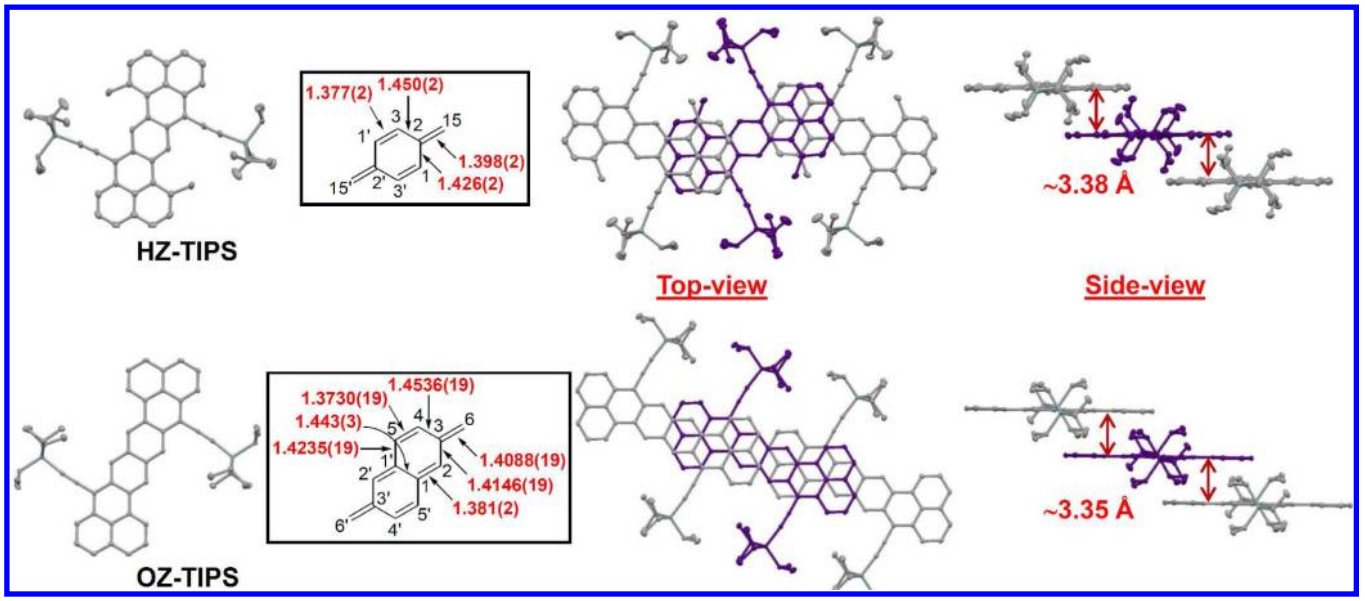

Figure 11. X-ray single-crystal structures of **HZ-TIPS** and **OZ-TIPS**, with bond length labeled for the central *p*-xylylene and 2,6-naphthodimethane units, and their top view and side view packing structures. Hydrogen atoms are omitted for clarity.

SI). The decomposition is likely due to addition of one or two oxygen molecules onto the heptazethrene or octazethrene backbone, as indicated by MALDI-TOF mass spectrometry (Figure S19–S20 in SI). The relatively good photostability of **OZ-TIPS** comes from the large extended delocalization of the biradicals and the kinetic blocking of the most reactive sites by TIPS groups.

3. CONCLUSION

In summary, kinetically blocked heptazethrene (**HZ-TIPS**) and octazethrene (**OZ-TIPS**) were prepared by a new synthetic approach. The attachment of the TIPS group at the most reactive site efficiently stabilizes the otherwise unstable biradicals. Both compounds show good stability both in the solid state and in solution due to kinetic blocking, which is important for their practical applications. Their electronic structures in the ground state were systematically investigated by a series of experimental methods assisted by DFT calculations. Steady-state absorption spectroscopic measurements disclosed the distinguished difference of the band structure between the open-shell **OZ-TIPS** and the closed-shell **HZ-TIPS**. Transient absorption and fluorescence spectra provided further information on the excited state lifetime, which again showed obvious difference between the open-shell and closed-shell structure. VT NMR, ESR, and SQUID were used to probe the magnetic properties, and the observed paramagnetism for the open-shell **OZ-TIPS** can be explained by the thermally excited singlet-to-triplet transition, which is an important feature of the singlet biradicaloids. More importantly, the singlet–triplet energy gap can be evaluated by VT ESR and SQUID experiments. FT-Raman spectroscopy was used to further probe the ground-state electronic structure. The quinoidal resonance form and the aromatic biradical resonance form can be nicely distinguished in their vibrational spectra, and even the singlet–triplet transition can be followed by the VT Raman measurements. Unrestricted symmetry-broken DFT calculations were used to understand the electronic structure and singlet biradical character. X-ray crystallographic analysis provided further information about the bond length, which is closely related to the ground-state electronic structure. Both compounds form a closely packed 1D infinite chain in single crystals via $\pi-\pi$ stacking, indicating their potential applications for ambipolar field effect transistors and spintronics. In addition, both compounds show large TPA cross sections, which is in agreement with theoretical predictions on the open-shell singlet biradicaloids. The large TPA response and good stability of these new compounds indicate their potential applications in nonlinear optics. By collecting all these experimental data and theoretical calculations, a clear picture of the ground state structure can be figured out: the **HZ-TIPS** has a closed-shell ground state while the higher order **OZ-TIPS** has an open-shell singlet biradical ground state. Remarkably, the singlet biradical character y = 0.56 for **OZ-TIPS** was obtained by a combination of the OPA, TPA, and SQUID data.

In contrast to our previously reported open-shell heptazethrene diimide (**HZ-DI**),[17] the **HZ-TIPS** has a closed-shell ground state, although it has the same heptazethrene core. This can be explained by the relatively large energy gap of the latter, indicating that a small energy gap is crucial for an open-shell ground state structure. It is noteworthy that the first stable octazethrene derivative **OZ-TIPS** was synthesized, which has been pursued by chemists for a long time. The design concept and the new synthetic strategy starting from the corresponding diketone likely can be applied to the synthesis of other stable open-shell polycyclic hydrocarbons or hybrid structures. The characterization methods reported here can be regarded as a comprehensive and systematical approach to investigate singlet biradicaloids in the future.

4. EXPERIMENTAL SECTION

The synthetic details and the general characterization methods (e.g., NMR and MS) are described in the Supporting Information.

Steady-state UV–vis absorption and fluorescence spectra were recorded on a Shimadzu UV-1700 spectrometer and a RF-5301 fluorometer, respectively.

The electrochemical measurements were carried out in anhydrous DCM with 0.1 M Bu_4NPF_6 as the supporting electrolyte at a scan rate of 0.05 V/s at room temperature under the protection of nitrogen. A gold disk was used as working electrode, platinum wire was used as

dx.doi.org/10.1021/ja304618v | J. Am. Chem. Soc. 2012, 134, 14913–14922

counting electrode, and Ag/AgCl (3 M KCl solution) was used as reference electrode. The potential was externally calibrated against the ferrocene/ferrocenium couple.

Continuous wave X-band ESR spectra were obtained with a Bruker ELEXSYS E500 spectrometer using a variable-temperature Bruker liquid nitrogen cryostat.

A superconducting quantum interference device magnetometer MPMS-XL was used for the magnetic characterization. The temperature-dependent magnetic susceptibility (χ_{mol}) was measured for the **HZ-TIPS** and **OZ-TIPS** samples under a constant magnetic field of 1000 Oe in the temperature range of 5−380 K.

FT−Raman spectra were measured using an FT−Raman accessory kit (FRA/106−S) of a Bruker Equinox 55 FT−IR interferometer. A continuous-wave Nd−YAG laser working at 1064 nm was employed for excitation, at a laser power in the sample not exceeding 30 mW. A germanium detector operating at liquid nitrogen temperature was used. Raman scattering radiation was collected in a back-scattering configuration with a standard spectral resolution of 4 cm^{-1}. 2000 scans were averaged for each spectrum. A variable-temperature cell Specac P/N 21525, with interchangeable pairs of quartz windows, was used to record the FT-Raman spectra at different temperatures. The variable temperature cell consists of a surrounding vacuum jacket (0.5 Torr), and combines a refrigerant Dewar and a heating block as the sample holder. It is also equipped with a copper constantan thermocouple for temperature monitoring between −170 and 150 °C. Samples were inserted into the heating block part or the Dewar/cell holder assembly in the form of pure solids dispersed in KBr pellets, and Raman spectra were recorded after waiting for thermal equilibrium in the sample. The samples in KBr pellets were prepared in an oxygen and water-free bag.

The femtosecond time-resolved transient absorption spectrometer used for this study consisted of a femtosecond optical parametric amplifier (Quantronix, Palitra-FS) pumped by a Ti:sapphire regenerative amplifier system (Quantronix, Integra-C) operating at 1 kHz repetition rate and an accompanying optical detection system. The generated OPA pulses had a pulse width of ∼100 fs and an average power of 1 mW in the range 450−800 nm, which were used as pump pulses. White light continuum (WLC) probe pulses were generated using a sapphire window (2 mm thick) by focusing of small portion of the fundamental 800 nm pulses, which were picked off by a quartz plate before entering into the OPA. The time delay between pump and probe beams was carefully controlled by making the pump beam travel along a variable optical delay (Newport, ILS250). Intensities of the spectrally dispersed WLC probe pulses were monitored by miniature spectrograph (OceanOptics, USB2000+). To obtain the time-resolved transient absorption difference signal (ΔA) at a specific time, the pump pulses were chopped at 25 Hz and absorption spectra intensities were saved alternately with or without pump pulse. Typically, 6000 pulses were used to excite samples and to obtain the TA spectra at a particular delay time. The polarization angle between pump and probe beam was set at the magic angle (54.7°) using a Glan-laser polarizer with a half-wave retarder to prevent polarization-dependent signals. The cross-correlation fwhm in the pump−probe experiments was less than 200 fs, and the chirp of WLC probe pulses was measured to be 800 fs in the 400−800 nm regions. To minimize chirp, all reflection optics were used in the probe beam path, and a quartz cell of 2 mm path length was employed. After completing each set of fluorescence and TA experiments, the absorption spectra of all compounds were carefully checked to rule out the presence of artifacts or spurious signals arising from, for example, degradation or photo-oxidation of the samples in question.

Time-resolved fluorescence lifetime experiments were performed by the TCSPC technique. As an excitation light source, we used a homemade cavity-dumped Ti:sapphire oscillator, which provides a high repetition rate (200−400 kHz) of ultrashort pulses [100 fs at full width at half-maximum (fwhm)] pumped by a continuous wave (cw) Nd-YVO_4 laser (Coherent, Verdi). The output pulse of the oscillator was frequency-doubled by a 1 mm thickness of a second harmonic crystal (barium borate, BBO, CASIX). The fluorescence was collected by a microchannel plate photomultiplier (MCP-PMT, Hamamatsu, R3809U-51) with a thermoelectric cooler (Hamamatsu, C4878) connected to a TCSPC board (Becker & Hickel SPC-130). The overall instrumental response function was about 25 ps (fwhm). A vertically polarized pump pulse by a Glan-laser polarizer irradiated samples, and a sheet polarizer, set at an angle complementary to the magic angle (54.7°), was placed in the fluorescence collection path to obtain polarization-independent fluorescence decays.

The two-photon absorption spectrum was measured in the NIR region using the open-aperture Z-scan method with 130 fs pulses from an optical parametric amplifier (Light Conversion, TOPAS) operating at a repetition rate of 3 kHz generated from a Ti:sapphire regenerative amplifier system (Spectra-Physics, Hurricane). After passing through a 10 cm focal length lens, the laser beam was focused and passed through a 1 mm quartz cell. Since the position of the sample cell could be controlled along the laser beam direction (z axis) using the motorcontrolled delay stage, the local power density within the sample cell could be simply controlled under constant laser intensity. The transmitted laser beam from the sample cell was then detected by the same photodiode as used for reference monitoring. The on-axis peak intensity of the incident pulses at the focal point, I_0, ranged from 40 to 60 GW cm^{-2}. For a Gaussian beam profile, the nonlinear absorption coefficient can be obtained by curve fitting of the observed open-aperture traces $T(z)$ with the following equation

$$T(z) = 1 - \frac{\beta I_0(1 - e^{-\alpha_0 l})}{2\alpha_0[1 + (z/z_0)^2]}$$

where α_0 is the linear absorption coefficient, l is the sample length, and z_0 is the diffraction length of the incident beam. After the nonlinear absorption coefficient has been obtained, the TPA cross section $\sigma^{(2)}$ of one solute molecule (in units of GM, where 1 GM = 10^{-50} cm^4 s $photon^{-1}$ $molecule^{-1}$) can be determined by using the following relationship

$$\beta = \frac{10^{-3}\sigma^{(2)}N_A d}{h\nu}$$

where N_A is Avogadro's constant, d is the concentration of the compound in solution, h is Planck's constant, and ν is the frequency of the incident laser beam.

Theoretical calculations were carried out by using the Gaussian 09 suite of programs. The initial geometry optimization of **HZ-TIPS** and **OZ-TIPS** was performed with the UCAM-B3LYP level of theory on the singlet state and the Handy and co-workers' long-range corrected version of B3LYP 6-31G*, and all electron basis sets were employed for all atoms.[26a,31] The resulting DFT solution (singlet "closed-shell": zero spin density on all atoms) was further tested for its stability with the STABLE=OPT keyword.[26b] A spin symmetry broken DFT solution was found with lower energy. Then the Guess=Read keyword was used to perform the optimization at the UCAM-B3LYP level (singlet open shell). Frequency calculations were conducted to ensure that these structures are indeed local minima. To simplify calculation, the triisopropylsilyl groups are replaced by triethylsilyl units.

■ ASSOCIATED CONTENT

Supporting Information

Synthetic procedures and characterization data of all new compounds, steady-state and time-resolved fluorescence spectra, Z-scan curves, photostability test details, and crystallographic data. This material is available free of charge via the Internet at http://pubs.acs.org.

■ AUTHOR INFORMATION

Corresponding Author

dongho@yonsei.ac.kr; osuka@kuchem.kyoto-u.ac.jp; casado@uma.es; msedingj@nus.edu.sg; chmwuj@nus.edu.sg

Notes

The authors declare no competing financial interest.

■ ACKNOWLEDGMENTS

J.W. acknowledges the financial support from the BMRC-NMRC grant (no. 10/1/21/19/642), MOE Tier 2 grant (MOE2011-T2-2-130), and A*STAR IMRE core funding (IMRE/10-1P0509). The work at Yonsei University was supported by WCU (World Class University) programs (*R*32-2010-10217-0) and an AFSOR/APARD grant (no. FA2386-09-1-4092). K.-W.H. acknowledges the financial support from KAUST. We thank Ji'En Wu and Yanhui Han for their kind assistance on the NMR analysis and Prof. Yuan-Chung Cheng for useful discussion.

■ REFERENCES

(1) (a) Rajca, A. *Chem. Rev.* **1994**, *94*, 871−893. (b) Morita, Y.; Suzuki, K.; Sato, S.; Takui, T. *Nat. Chem.* **2011**, *3*, 197−204. (c) Lambert, C. *Angew. Chem., Int. Ed.* **2011**, *50*, 1756−1758. (d) Sun, Z.; Wu, J. *J. Mater. Chem.* **2012**, *22*, 4151−4160. (e) Sun, Z.; Ye, Q.; Chi, C.; Wu, J. *Chem. Soc. Rev.* **2012**, DOI: 10.1039/c2cs35211G.

(2) Kamada, K.; Ohta, K.; Kubo, T.; Shimizu, A.; Morita, Y.; Nakasuji, K.; Kishi, R.; Ohta, S.; Furukawa, S.; Takahashi, H.; Nakano, M. *Angew. Chem., Int. Ed.* **2007**, *46*, 3544−3546.

(3) (a) Chikamatsu, M.; Mikami, T.; Chisaka, J.; Yoshida, Y.; Azumi, R.; Yase, K. *Appl. Phys. Lett.* **2007**, *91*, 043506. (b) Chase, D. T.; Fix, A. G.; Kang, S. J.; Rose, B. D.; Weber, C. D.; Zhong, Y.; Zakharov, L. N.; Lonergan, M. C.; Nuckolls, C.; Haley, M. M. *J. Am. Chem. Soc.* **2012**, *134*, 10349−10352. (c) Nishida, J.; Tsukaguchi, S.; Yamashita, Y. *Chem.—Eur. J.* **2012**, *18*, 8964−8970.

(4) Yazyev, O.; Katsnelson, M. I. *Phys. Rev. Lett.* **2008**, *100*, 047209.

(5) Morita, Y.; Nishida, S.; Murata, T.; Moriguchi, M.; Ueda, A.; Satoh, M.; Arifuku, K.; Sato, K.; Takui, T. *Nat. Mater.* **2011**, *10*, 947−951.

(6) (a) Son, Y. W.; Cohen, M. L.; Louie, S. G. *Nature* **2006**, *444*, 347−349. (b) Son, Y. W.; Cohen, M. L; Louie, S. G. *Phys. Rev. Lett.* **2006**, *97*, 216803. (c) Kim, W. Y.; Kim, K. S. *Nat. Nanotechnol.* **2008**, *3*, 408−412.

(7) (a) Thiele, J.; Balhorn, H. *Chem. Ber.* **1904**, *37*, 1463. (b) Flynn, C. R.; Michl, J. *J. Am. Chem. Soc.* **1974**, *96*, 3280−3288. (c) Montgomery, L. K.; Huffman, J. C.; Jurczak, E. A.; Grendze, M. P. *J. Am. Chem. Soc.* **1986**, *108*, 6004−6011. (d) Chase, D. T.; Rose, B. D.; McClintock, S. P.; Zakharov, L. N.; Haley, M. M. *Angew. Chem., Int. Ed.* **2011**, *50*, 1127−1130. (e) Zeng, Z.; Sung, Y. M.; Bao, N.; Tan, D.; Lee, R.; Zafra, J. L.; Lee, B. S.; Ishida, M.; Ding, J.; Lopez Navarrete, J. T.; Li, Y.; Zeng, W. D.; Kim, D.; Huang, K.-W.; Webster, R. D.; Casado, J.; Wu, J. *J. Am. Chem. Soc.* **2012**, DOI: 10.1021/ja3050579.

(8) (a) Kolc, J.; Michl, J. *J. Am. Chem. Soc.* **1970**, *92*, 4147−4148. (b) Iwashita, S.; Ohta, E.; Higuchi, H.; Kawai, H.; Fujiwara, K.; Ono, K.; Takenaka, M.; Suzuki, T. *Chem. Commun.* **2004**, 2076−2077. (c) Shimizu, A.; Tobe, Y. *Angew. Chem., Int. Ed.* **2011**, *50*, 6906−6910.

(9) (a) Reid, D. H. *Chem. Ind.* **1956**, 1504−1505. (b) Gerson, F. *Helv. Chim. Acta* **1966**, *49*, 1463−1472. (c) Goto, K.; Kubo, T.; Yamamoto, K.; Nakasuji, K.; Sato, K.; Shiomi, D.; Takui, T.; Kubota, M.; Kobayashi, T.; Yakusi, K.; Ouyang, J.-Y. *J. Am. Chem. Soc.* **1999**, *121*, 1619−1620. (d) Itkis, M. E.; Chi, X.; Cordes, A. W.; Haddon, R. C. *Science* **2002**, *296*, 1443−1445.

(10) (a) Ohashi, K.; Kubo, T.; Masui, T.; Yamamoto, K.; Nakasuji, K.; Takui, T.; Kai, Y.; Murata, I. *J. Am. Chem. Soc.* **1998**, *120*, 2018−2027. (b) Kubo, T.; Sakamoto, M.; Akabane, M.; Fujiwara, Y.; Yamamoto, K.; Akita, M.; Inoue, K.; Takui, T.; Nakasuji, K. *Angew. Chem., Int. Ed.* **2004**, *43*, 7474−6479. (c) Kubo, T.; Shimizu, A.; Sakamoto, M.; Uruichi, M.; Yakushi, K.; Nakano, M.; Shiomi, D.; Sato, K.; Takui, T.; Morita, Y.; Nakasuji, K. *Angew. Chem., Int. Ed.* **2005**, *44*, 6564−6568. (d) Shimizu, A.; Uruichi, M.; Yakushi, K.; Matsuzaki, H.; Okamoto, H.; Nakano, M.; Hirao, Y.; Matsumoto, K.; Kurata, H.; Kubo, T. *Angew. Chem., Int. Ed.* **2009**, *48*, 5482−5486. (e) Shimizu, A.; Kubo, T.; Uruichi, M.; Yakushi, K.; Nakano, M.; Shiomi, D.; Sato, K.; Takui, T.; Hirao, Y.; Matsumoto, K.; Kurata, H.; Morita, Y.; Nakasuji, K. *J. Am. Chem. Soc.* **2010**, *132*, 14421−14428. (f) Shimizu, A.; Hirao, Y.; Matsumoto, K.; Kurata, H.; Kubo, T.; Uruichi, M.; Yakushi, K. *Chem. Commun.* **2012**, *48*, 5629−5631.

(11) Konishi, A.; Hirao, Y.; Nakano, M.; Shimizu, A.; Botek, E.; Champagne, B.; Shiomi, D.; Sato, K.; Takui, T.; Matsumoto, K.; Kurata, H.; Kubo, T. *J. Am. Chem. Soc.* **2010**, *132*, 11021−11023.

(12) (a) Bendikov, M.; Duong, H. M.; Starkey, K.; Houk, K. N.; Carter, E. A.; Wudl, F. *J. Am. Chem. Soc.* **2004**, *126*, 7416−7417. (b) Jiang, D.-E.; Dai, S. *J. Phys. Chem. A* **2008**, *112*, 332−335.

(13) (a) Jiang, D.-E.; Sumpter, B. G.; Dai, S. *J. Chem. Phys.* **2007**, *127*, 124703. (b) Yao, J.; Chi, C.; Wu, J.; Loh, K.-P. *Chem.—Eur. J.* **2009**, *15*, 9299−9302. (c) Zhang, K.; Huang, K.-W.; Li, J.; Luo, J.; Chi, C.; Wu, J. *Org. Lett.* **2009**, *11*, 4854−4857. (d) Li, J.; Zhang, K.; Zhang, X.; Huang, K.-W.; Chi, C.; Wu, J. *J. Org. Chem.* **2010**, *75*, 856−863. (e) Zhang, X.−J.; Li, J.; Qu, H.; Chi, C.; Wu, J. *Org. Lett.* **2010**, *12*, 3946−3949. (f) Li, J.; Jiao, C.; Huang, K.-W.; Wu, J. *Chem.—Eur. J.* **2011**, *17*, 14672−14680. (g) Li, J.; Chang, J.; Tan, P.; Jiang, H.; Chen, X.; Chen, Z.; Zhang, J.; Wu, J. *Chem. Sci.* **2012**, *3*, 846−850.

(14) (a) Nakano, M.; Kishi, R.; Takebe, A.; Nate, M.; Takahashi, H.; Kubo, T.; Kamada, K.; Ohta, K.; Champagne, B.; Botek, E. *Comput. Lett.* **2007**, *3*, 333−338. (b) Yoneda, K.; Nakano, M.; Fukui, H.; Minami, T.; Shigeta, Y.; Kubo, T.; Botek, E.; Champagne, B. *ChemPhysChem* **2011**, *12*, 1697−1707.

(15) (a) Clar, E.; Lang, K. F.; Schulz-Kiesow, H. *Chem. Ber.* **1955**, *88*, 1520−1527. (b) Staab, H. A.; Nissen, A.; Ipaktschi, J. *Angew. Chem., Int. Ed. Engl.* **1968**, *7*, 226−226. (c) Mitchell, R. H.; Sondheimer, F. *Tetrahedron* **1970**, *26*, 2141−2150. (d) Umeda, R.; Hibi, D.; Miki, K.; Tobe, Y. *Org. Lett.* **2009**, *11*, 4104−4106. (e) Wu, T. C.; Chen, C. H.; Hibi, D.; Shimizu, A.; Tobe, Y.; Wu, Y. T. *Angew. Chem., Int. Ed.* **2010**, *49*, 7059−7062. (f) Sun, Z.; Huang, K.-W.; Wu, J. *Org. Lett.* **2010**, *12*, 4690−4693.

(16) Clar, E.; Macpherson, I. A. *Tetrahedron* **1962**, *18*, 1411−1416.

(17) Sun, Z.; Huang, K.-W.; Wu, J. *J. Am. Chem. Soc.* **2011**, *133*, 11896−1199.

(18) Erünliü, R. K. *Liebigs Ann. Chem.* **1969**, *721*, 43−47.

(19) Merlet, S.; Birau, M.; Wang, Z. Y. *Org. Lett.* **2002**, *4*, 2157−2159.

(20) Bailey, R. J.; Card, P. J.; Shechter, H. *J. Am. Chem. Soc.* **1983**, *105*, 6096−6103.

(21) (a) Weil, T.; Vosch, T.; Hofkens, J.; Peneva, K.; Müllen, K. *Angew. Chem., Int. Ed.* **2010**, *49*, 9068−9093. (b) Anthony, J. *Angew. Chem. Int. Ed.* **2008**, *47*, 452−483.

(22) Motta, S. D.; Negri, F.; Fazzi, D.; Castiglioni, C.; Canesi, E. V. *J. Phys. Chem. Lett.* **2010**, *1*, 3334−3339.

(23) Koide, T.; Furukawa, K.; Shinokubo, H.; Shin, J.-Y.; Kim, K. S.; Kim, D.-H.; Osuka, A. *J. Am. Chem. Soc.* **2010**, *132*, 7246−7247.

(24) Bleaney, B.; Bowers, K. D. *Proc. R. Soc. London Ser. A* **1952**, *214*, 451−465.

(25) (a) Ortiz, R. P.; Casado, J.; Hernández, V.; Navarrete, J. T. L.; Viruela, P. M.; Ortí, E.; Takimiya, K.; Otsubo, T. *Angew. Chem., Int. Ed.* **2007**, *46*, 9057−9061. (b) Casado, J.; Patchkovskii, S.; Zgierski, M. Z.; Hermosilla, L.; Sieiro, C.; Moreno Oliva, M.; López Navarrete, J. T. *Angew. Chem., Int. Ed.* **2008**, *47*, 1443−1447. (c) González, S. R.; Ie, Y.; Aso, Y.; López Navarrete, J. T.; Casado, J. *J. Am. Chem. Soc.* **2011**, *133*, 16350−16353.

(26) (a) Yanai, T.; Tew, D.; Handy, N. *Chem. Phys. Lett.* **2004**, *393*, 51−57. (b) Seeger, R.; Pople, J. A. *J. Chem. Phys.* **1977**, *66*, 3045−3050.

(27) Kamada, K.; Ohta, K.; Shimizu, A.; Kubo, T.; Kishi, R.; Takahashi, H.; Botek, E.; Champagne, B.; Nakano, M. *J. Phys. Chem. Lett.* **2010**, *1*, 937−940.

(28) Pawlicki, M.; Collins, H. A.; Denning, R. G.; Anderson, H. L. *Angew. Chem., Int. Ed.* **2009**, *48*, 3244−3266.

(29) Crystallographic data for **HZ-TIPS**: $C_{52}H_{60}Si_2$, M_w = 741.18; monoclinic; space group C_2/c; a = 18.548(6), b = 19.178(6), c = 13.920(5) Å, β = 122.838(4)°; V = 4160(2) Å^3; Z = 4; ρ_{calcd} = 1.183 Mg/m^3; R_1 = 0.0480 ($I > 2\sigma(I)$), wR_2 = 0.1398 (all data). CCDC No. 875408. X-ray-quality crystal was obtained by slow evaporation of the solution in toluene/heptane.

(30) Crystallographic data for **OZ-TIPS**: $C_{54}H_{58}Si_2$, M_w = 763.18; triclinic; space group $\bar{P}1$; a = 8.410(3) Å, b = 9.846(4) Å, c = 14.020(6) Å, α = 73.046(5)°, β = 77.078(5)°, γ = 87.083(5)°; V = 1082.1(8) Å^3; Z = 1; ρ_{calcd} = 1.171 Mg/m^3; R_1 = 0.0345 ($I > 2\sigma(I)$), wR_2 = 0.0947 (all data). CCDC No. 875409. X-ray-quality crystal was obtained by slow evaporation of the solution in toluene/THF/heptane.

(31) (a) Lee, C.; Yang, W.; Parr, R. G. *Phys. Rev. B* **1988**, *37*, 785−789. (b) Becke, A. D. *J. Chem. Phys.* **1993**, *98*, 5648−5652. (c) Ditchfie, R. W.; Hehre, J.; Pople, J. A. *J. Chem. Phys.* **1971**, *54*, 724−728. (d) Hehre, W. J.; Ditchfie, R.; Pople, J. A. *J. Chem. Phys.* **1972**, *56*, 2257−2261. (e) Harihara, P. C.; Pople, J. A. *Theor. Chim. Acta* **1973**, *28*, 213−222.